Microwaves and Functional Materials: A Novel Method to Continuously Detect Metal Ions in Water

Ilaria Frau, Stephen Wylie, Jeff Cullen, Olga Korostynska, Patrick Byrne and Alex Mason

Abstract Protecting water from chemical pollutants is a major societal goal. Metal ion dispersion from abandoned mines is a global concern and one of the principal causes of metal pollution in water. Toxic metals are a particular concern because they are not degraded by normal biogeochemical cycles and cause adverse environmental and human health effects even with low concentrations if there is long-term exposure. Current laboratory-based methods are not suitable for monitoring adequately water pollution in the environment. Consequently, it is necessary to develop and deploy new sensing systems to investigate water quality continuously. Microwave spectroscopy has been demonstrated as an effective method for offering continuous measurement of material properties, nevertheless, this method suffers from a lack of selectivity and sensitivity (Zarifi et al. Sens Actuators B Chem 255:1561–1568 (2018), [1]). This chapter presents a feasibility study using unique functionalised electromagnetic (EM) sensors for continuous monitoring of zinc in water. The reaction between Zn and a Bi_2O_3 based thick film that is screen-printed onto a planar interdigitated electrode (IDE) sensors starts within 30 s, and the adsorption equilibrium was attained within 10 min. The response is faster during the initial stage and slows as equilibrium is reached. Results show good linear correlations between C (capacitance), S_{11} (reflection coefficient) and Zn concentration. Also, the recovery time of sensors is evaluated to be 100–150 s demonstrating the sensors reusability and potential for continuous monitoring.

I. Frau · S. Wylie · J. Cullen · O. Korostynska
Faculty of Engineering and Technology, Liverpool John Moores University, Liverpool, UK

P. Byrne
Faculty of Science, Liverpool John Moores University, Liverpool, UK

A. Mason (✉)
Animalia AS, Norwegian Meat and Poultry Research Centre, Oslo, Norway
e-mail: alex.mason@animalia.no

Need for Research—Statement of a Problem

Water, especially freshwater, is an indispensable resource, but it is limited in quantity and in quality. Assuring a high quality of water and protecting it from chemical contamination is a major sustainable development goal [2, 3] that is becoming increasingly hard to achieve owing to factors such as climate change, overexploitation and contamination from agricultural and industrial activities.

Polluted drainage from both contemporary and historical mining and mine wastes are an issue of international concern that can result in significant water quality issues [4]. Point and diffuse sources determine the dispersion into the environment of toxic inorganic pollutants, mainly metals (zinc, lead, cadmium, copper, mercury, arsenic, etc.), in addition to problems associated with high sulphate concentrations and acidification of watercourses. Surface water, directly connected with groundwater [5], is the predominant route of dispersion of these toxic elements even at considerable distances from the source, with the consequent possibility to pollute drinking water supplies.

Metals are considered trace elements due to their presence in the environment at generally low concentrations (μg/l range to less than 100 mg/l). Their bioavailability is regulated by several physical and chemical factors, such as temperature, pH and consequent differential adsorption, phase association, thermodynamic equilibrium, complexation kinetics, and so forth [6].

Consequently, European and worldwide legislation has established environmental quality standard (EQS) for metals in surface water, which is the major route of dispersion of these pollutants. Table 1 summarises the EQS established by the UK Technical Advisory Group on the EU Water Framework Directive (UKTAG) [7] and US EPA (Environmental protection agency) [8] for toxic metals concentrations and sulphates (strongly related to them), and the typically investigated metal ion concentrations in mining catchment areas [9, 10].

Generally, the ionic metal form is considered the most toxic, although other weakly complexed species (oxides, hydroxides, and sulphates) and organic colloidal phases are also a cause for concern. The metal ionic form and its precipitation or sorption to other phases are related to the pH, the sorbate identity and concentration, the sorbent composition, and so forth [12].

Zinc (Zn) is a hazardous toxicant, which when present at high concentrations for a long-term, can cause such significant effects in humans as respiratory disorders, bronchiolar leukocytes, neuronal disorders [13]. Zinc levels in non-polluted waters range from 0.06 to 0.6 μg/l. In drinking water, it is typically around 10 μg/l but higher concentrations than 2 mg/l are found especially when the water passes through zinc pipes [14]. Globally, Zn in mine water ranges from <0.1 to >500 mg/l [10], failing the established EQS limit of 0.008–0.125 mg/l. The Water Framework Directive and the Clean Water Act, the main legal frameworks for the protection and the sustainable

Table 1 UK EQS for some metals and sulphates in surface water and global range concentrations from waters impacted by historical deep metal mining

Toxic metals	UK EQS (mg/l) for inland and other surface water [7, 11]	US EPA EQS (mg/l) for freshwater (acute and chronic) [8]	Global concentration ranges in polluted mining surface water (mg/l) [9]
Lead (Pb)	0.0072[a]	0.0015–0.065[b]	<0.0072–>12
Zinc (Zn)	0.008–0.125[b]	0.059–0.210[b]	<0.008–>500
Copper (Cu)	0.001–0.028[b]	0.017–0.034[b]	<0.001–>240
Cadmium (Cd)	0.00008–0.00025[a,b]	0.00066–0.0018[b]	<0.00008–>2.6
Iron (Fe)	1	0.3–1	<1–>1900
Sulphates (SO4)	400	250	<400–>16,000

[a]dissolved concentration (<0.45 μm)
[b]depending on the annual mean concentration of $CaCO_3$

use of freshwater resources respectively in Europe and in USA, [15] require new low-cost sensing systems for in situ monitoring, and managing water resources to minimise the environmental risk posed by mine drainage from active and abandoned mining complexes [16].

Current Methods for Metal Detection

Current methods for detecting Zn concentration (and the other toxic metals) in water are mainly laboratory-based. Examples include atomic absorption spectroscopy, inductively coupled plasma—optical emission spectrometry, inductively coupled plasma—mass spectrometry [17]. Although these methods can determine multi-metal concentrations with high selectivity and sensitivity with a low limit of detection, they have critical drawbacks. These bulky laboratory methods require sample preparation, costly chemicals and trained staff. They are unable to provide real-time and in situ measurements which limits the possibility to detect an unexpected event (i.e. the failure of a mine tailings dam spill) [18, 19] or to understand metal variations when environmental conditions change (i.e. during a flood event) [20]. Moreover, without a continuous in situ monitoring, traditional methods cannot give an answer to alterations of each metal concentration changes due to differences between high flow and low flow [21], variation in pH and temperature, presence or absence of hydrated iron oxide (HFO) on the riverbed in polluted mining areas [12, 22–24].

Water quality monitoring for emergency detection and management using advanced low-cost sensor technologies are essential for polluted water remediation. Accordingly, significant research is in progress for in situ and real-time measurements of heavy metal ions, and appreciable results have been reported using optical, electrochemical techniques and near-infrared spectroscopy [25–27].

Although these methods are sensitive and stable, they can also be cumbersome, time-consuming, expensive and laborious. Hence, the UN Agenda for Sustainable development calls for a low-cost sensing system for online and in situ monitoring [15]. Therefore, further work is needed to develop simple, reliable, and cost-effective techniques for remote detection of pollutants, to better understand the processes that regulate metal dispersion and allow for an emergency response to unexpected events.

F-EM Sensors as a Solution

A new and rapidly developing method capable of providing a continuous monitoring of metals in freshwater, namely Zn in this work, is an electromagnetic (EM) wave sensor system combined with functional materials, operating at microwave frequencies [28]. This method is highly adaptable and, depending on each scenario, can take the form of planar sensors [29–31], resonant cavities [32], flexible sensors [33], for example. Their design can be tailored to suit particular applications and is coupled with reliability and cost-efficiency.

Microwave planar printed patterns, in particular, have been increasingly used for various sensing applications due to their versatility, flat profile, low weight, simplicity, low-cost [34]. In fact, planar sensors can be easily integrated with microfluidic techniques [35], nanostructures [36], thin and thick films [37], for specific sensing purposes.

The principle of microwave spectroscopy is based on the singular interaction between incident waves at specific frequencies with the properties of the analyte presented to the sensing structure (such as conductivity, capacitance, resistance, inductance and permittivity, as well as temperature, chemical structure, molecular composition, etc.), as illustrated in Fig. 1a. The change in the S_{11} reflection coefficient can be linked to the composition and concentration of the measured solution (Fig. 1b, c). Accordingly, permittivity (ε_r) as defined in (1) relates to a material's ability to transmit an electric field and is a complex value which varies with changing frequency and accounts for both the energy stored by a material and any losses of energy which might occur.

$$\varepsilon_r = \varepsilon' - j\varepsilon'' \tag{1}$$

The response of the sensor manifests itself as a resonant frequency change or attenuation of the signal [38].

Microwave spectroscopy, however, suffers from a lack of selectivity, specificity and sensitivity. A feasible solution to this problem is to integrate EM sensors with functional materials.
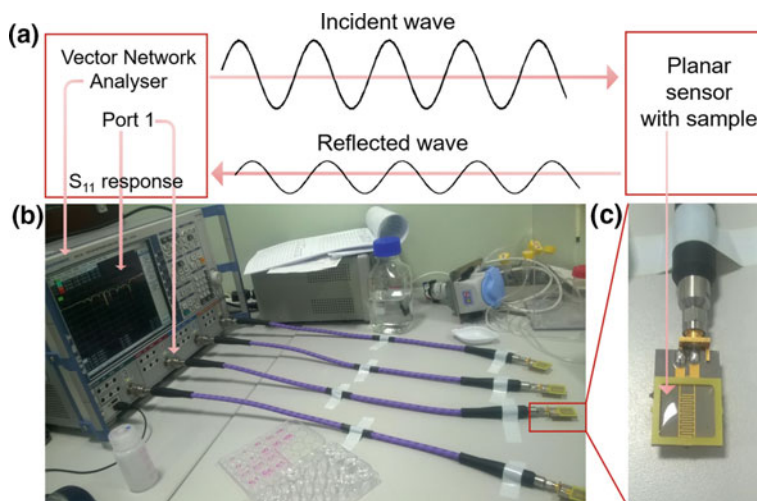
Fig. 1 (**a**) Scheme which describes the reflected signal (S_{11}) at discrete frequencies as spectrum response (**b**) with the unique interaction of the incident wave with the sample under test (**c**)

Synergy with Functional Material

Microwave spectroscopy connected with the appropriate sensing system could be able to analyse changes in properties and composition of several materials and components. Notably, the lack of selectivity is a limitation in designing a microwave sensor for a particular purpose [39]. A possible solution are planar waveguide-based chemical sensors [40]. The synergy between microwave sensing technology and chemical coatings provides interesting advantages in the field of water quality monitoring and is consequently a promising area of research and development [34, 41].

By functionalising planar EM sensors with certain sensitive materials, it is possible to obtain the desired sensitivity and/or selectivity to one or more specific analytes. This can be achieved not only with the adoption of the right sensing material but also by choosing the right thickness of the functional film and sensor geometry [42, 43]. Moreover, coatings prevent short-circuiting and oxidation when the sensor is exposed to a water sample.

The principle of using a distinct chemical coating and the interaction with selected analytes is based on the variation in the resulting electrical impedance due to the change in complex permittivity. The spectral response due to this variation will generate amplitude and/or frequency changes at specific frequency ranges [34].

Considerable progress has been made in the last decade in developing chemosensors that are able to distinguish specific metal ions, such as Zn, by using different functional materials including synthetic and biological receptors [44], zeolites, inorganic oxides [45], organic polymers, biological materials [46] and hybrid ion-exchangers [47].

Screen-Printing Technology

The goal of a cheap, sensitive and selective device to monitor metal-impacted water is achievable by the integration of chemical coatings and planar sensors using screen-printing technology [48]. These are known for their flexibility and cost-effective mass production [49]. Screen-printing is a technique where a viscous ink (0.1 to 10 Pa s) based on functional materials is set in a screen blocking layer with a stencil (a negative of the image to be printed), which defines an open area of the mesh. A squeegee is moved across the screen and the ink passes through the mesh and a thick film is created [50].

The main advantages of screen-printing as the application method for functional materials is the high diversity of materials that can be processed at low cost, and the possibility of printing a combination of different materials onto the same substrate [51]. Designing functionalised sensors with the best-suited architecture will help to increase the selective identification of multi-metal ions and other pollutants simultaneously present in water [52].

Screen-printed electrodes coupled with specific sensing materials are an attractive option for adapting diverse sensing systems to a particular purpose [50]. The screen-printing technique is used to form a thick film on top of microwave sensors and increase, by chemical or physical reaction, the sensitivity, specificity and selectivity between the EM waves and the analyte. Thick films are rugged, reproducible, inexpensive and have also been identified as useful for integration into remote monitoring systems [48, 51].

Among functional chemical compounds, bismuth (Bi) has been largely used in the last 20 years in a number of approaches for detecting metals in water. Furthermore, bismuth nanoparticles have shown in several experiments to have superior sensing characteristics compared to the Bi film electrode for detecting metals in water, mostly using electrochemical methods [53–56]. Moreover, nanomaterials as inorganic oxide compositions are considered to be advantageous, owing to their strong adsorption and rapid electron transfer kinetic [25, 45]. Nanostructured metal oxides are also interesting for their nano-morphological, functional biocompatible, non-toxic and catalytic properties. In this work, interdigitated electrodes sensors are functionalised with β-Bi_2O_3 based coatings.

The purpose of this chapter is to evaluate the feasibility of using functionalised EM planar sensors (f-EM sensors) for continuously monitoring the concentration of Zn in polluted mine water. The response time was measured for β-Bi_2O_3 based sensing film using two sensing techniques: microwave spectroscopy and capacitance measurements. Moreover, the sensors' stability and reusability were assessed by measuring their recovery time.

Experimental Setup

The time of reaction between Zn solutions and the β-Bi_2O_3 based coating, on two gold eight-pair IDE sensors on a planar PTFE (polytetrafluoroethylene) substrate was analysed using microwave and electric techniques, by measuring respectively the reflection coefficient (at 10 MHz–10 GHz) and the capacitance (at 30–200 kHz).

Fabrication of the Screen-Printed Sensors

Generally, for the development of a low-cost printable paste mixture of the desired viscosity three components are necessary: (1) a principal functional material, (2) an organic binder and (3) an organic volatile solvent. These last two components work as a matrix for developing the correct viscosity of a paste to be printed over the planar sensors.

Two sets of Au eight–pair IDE sensors were functionalised using a semi-automatic screen printer (Super Primex). A series of Ag eight-pair IDE patterns were also screen-printed in situ at LJMU on microscope slide substrates using a Silver conductor (Dupont 5064H) for a secondary cheaper development and deployment of the coatings and an initial characterization of them. Repeatability and reproducibility of the IDEs were evaluated by impedance measurements (Cp, Rp, Z).

β-Bi_2O_3 nanopowder $90 < \Phi < 210$ nm particle size, characterised by tetragonal phase and space group P 42_1 c (114), (Sigma-Aldrich 637017) was used as the principal chemical for creating the paste mixture to form the thick film. 92.5 wt% bismuth oxide nanopowders were mixed with 7.5 wt% of a polymer (Butvar B98) used as a binder, and a suitable amount of ethylene glycol butyl ether (solvent) to form the paste. The thickness of the β-Bi_2O_3 based thick film was increased by multiple screen-printing, with the set of two sensors having 4 and 6 layers printed, with suitable curing of the layers in an oven at 170º C for 1 h between each print. The schematic diagram of the screen-printing process is shown in Fig. 2.

The thickness of the final films was measured using an electronic micrometer (TESA Micromaster), a digital vernier caliper (AOS Absolute Digimatic) and a surface profiler (Taylor Hobson—Form Talysurf 120), resulting in average of 40 and 60 μm respectively for 4 and 6 layers. Morphological properties and elemental composition were analysed before and after Zn detection using a scanning electron microscope (SEM), model FEI—Quanta 200 and a X-Ray fluorescence analyser (XRF), model INCA-X-act—Oxford Instruments. Coating repeatability and reproducibility was measured through absorbance measurements of screen-printed microscope slides with β-Bi_2O_3 based paste mixtures prepared on distinct days. These measurements were performed with a UV-Vis Spectrophotometer (Jenway 7315) as shown in Fig. 3.
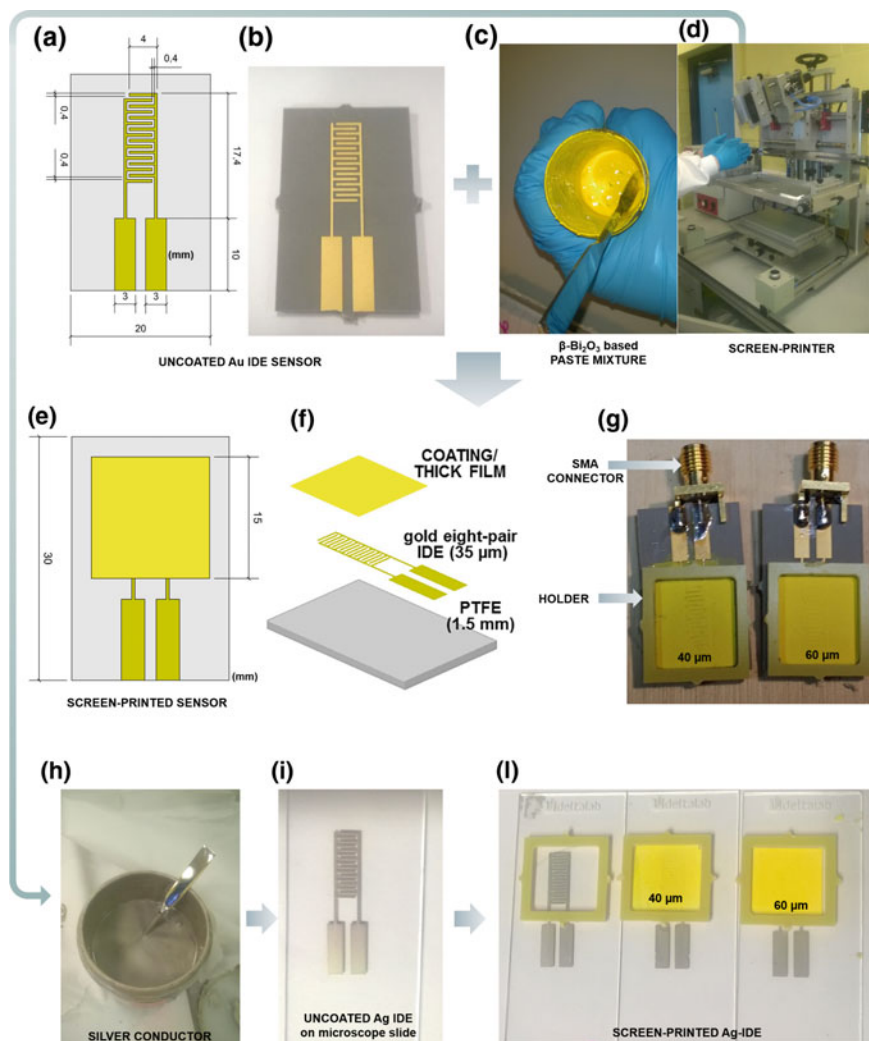
Fig. 2 Scheme which summaries the integration of functional materials with planar sensors by using screen-printing technology and consequent production of thick films. Uncoated Au IDE sensors (**a**, **b**) were screen-printed using a β-Bi$_2$O$_3$ based paste mixture (**c**) and a semi-automatic screen-printer (**d**). The finished coated sensors have 40 and 60 μm thicknesses (**e**–**g**). In-situ Ag-IDE were screen-printed on microscope slides using a silver conductor paste (**d**, **h**, **i**) and covered as described for the Au IDE sensors (**l**). The front and rear view along with the dimension of the sensor and the sensing area are shown in (**a**), (**e**) and (**f**)

Fig. 3 Repeatability of coating method was assessed using UV-vis spectroscopy

Table 2 pH and conductivity of the zinc solutions

Zn solutions		
Zn concentration (mg/l)	pH	Conductivity
0	7.36	1.1 µS/cm
1	3.78	134.4 µS/cm
10	2.60	1.282 mS/cm
25	2.42	3.36 mS/cm
50	1.99	6.52 mS/cm
100	1.97	13.02 mS/cm

Sample Preparation

Six samples with different zinc concentrations (0, 1, 10, 25, 50, 100 mg/l) were prepared by dissolving a defined volume of Zn 1,000 ppm ICP standard solution certified (Sigma-Aldrich 18562) in deionised water. The chemical and physical parameters (pH and conductivity, Table 1) for all the samples were evaluated at constant temperature using a multi-parameter probe (PCE-PHD 1). All measurements were performed in an air-conditioned environment at a constant temperature of 18.5° C (Table 2).

Measurement Setup

Functionalised Au IDE sensors coated with the β-Bi_2O_3 based film with 40 and 60 µm thicknesses were connected to a Rohde and Schwarz ZVA 2.4 VNA (Vector Network Analyser) via a coaxial cable (Fig. 4a). In this work Molex edge mount
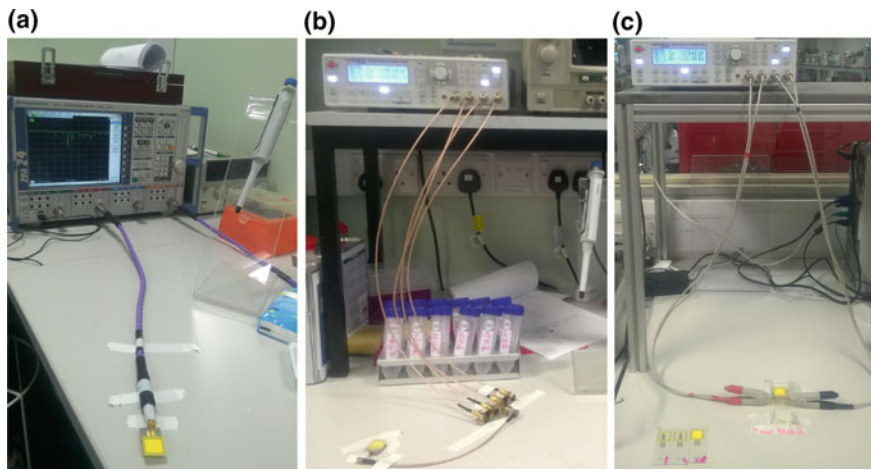
Fig. 4 Configuration of the EM measurements with **a** VNA connected via coaxial cable with a Au eight-pair IDE coated with β-Bi$_2$O$_3$ based coating. Set up of the HAMEG programmable LCR bridge connected to a coated Au IDE planar sensor (**b**) and to a coated Ag eight-pair IDE on microscope slide through a R&S HZ184 K measurable cable (**c**)

connectors were used. The reflection coefficient (S$_{11}$) relative to the 50 Ω impedance of the VNA was measured with a one-port configuration in the 10 MHz to 15 GHz frequency range, producing a detailed spectrum with 60,000 discrete points. For each measurement, 400 µl of Zn solution was dispensed onto the sensor using a pipette, with the solution held in place by a specific holder (Fig. 2g).

Each solution was tested (n = 3) for 30 min with both sensors. This technique permits a continuous measurement and the output was extracted every 30 s to monitor any time variation in the interaction between the coatings (40 and 60 µm) and the Zn solutions.

The sensor capacitance (C) and their interaction with Zn samples was measured using a programmable LCR bridge HAMEG 8118 configured with a bespoke coaxial probe (Fig. 4b) at the frequency range between 30 Hz and 200 kHz. Coated Ag-IDE screen-printed on microscope slide were connected with the LCR bridge through a R&S HZ184 K measurable cable (Fig. 4c). For consistency, 400 µl volume water samples were used.

Once the sensors' output in all frequency ranges was analysed using both Au and Ag electrodes, 150 Hz was selected to determine the variation in capacitance over 30 min, with a measurement recorded every 5 s. The purpose of doing this was to assess changes in electrical properties and the consequent reaction between the coated sensors and Zn solutions. All Zn samples were measured at the same temperature to eliminate possible effect of the temperature on the microwave spectra [36].

Table 3 The percentage of adsorption between β-Bi$_2$O$_3$ based film and Zn

Zn concentration (mg/l)	After 5 min		After 10 min		After 30 min	
	Conc.	%	Conc.	%	Conc.	%
0	0	0	0	0	0	0
1	0.96	4.1	0.938	6.2	0.938	6.2
10	9.6	4	9.39	6.1	9.4	6
50	48.3	3.5	47.3	5.4	47.25	5.5
100	96.7	3.3	94.9	5.1	94.8	5.2

Adsorption Experiment

The percentage of adsorption between adsorbent (β-Bi$_2$O$_3$) and adsorbate (Zn^{2+}) was estimated by measuring the difference of the initial concentration of each Zn solution and the concentration after the adsorption, by modifying the procedure described by Dada et al. [57] for simulating the capability of the coating to adsorb Zn ions. 0.02 g of the thick film (printed on a microscope slide) was put in a plastic container with 20 ml of each Zn solution (0, 1, 10, 50, 100 mg/l). The concentrations in the solution after the adsorption was measured after 5, 10 and 30 min.

The percentage of adsorption was evaluated using Eq. (2).

$$\% \ adsorption = \frac{c_i - c_e}{c_i} \times 100 \tag{2}$$

where C$_i$ is the Zn concentration before the adsorption and C$_e$ is the Zn concentration after the adsorption.

Results and Discussion

Results obtained with both electric and microwave measurements show how the reaction between Zn and the coating is observed to commence within 30 s of exposure and reach an adsorption equilibrium time within 600 s (10 min). At this point, the measurement of the percentage of adsorption demonstrates that approximately 4% of zinc is adsorbed on the coating about after 5 min and 6% after 10 min, reaching an adsorption equilibrium (Table 3).

Likewise, with the higher concentrations (50 and 100 mg/l), the percentage of adsorption is slightly reduced presumably due to the lower pH (<2, see Table 1). As a matter of fact, the adsorption of cations on metal-oxide minerals in the natural
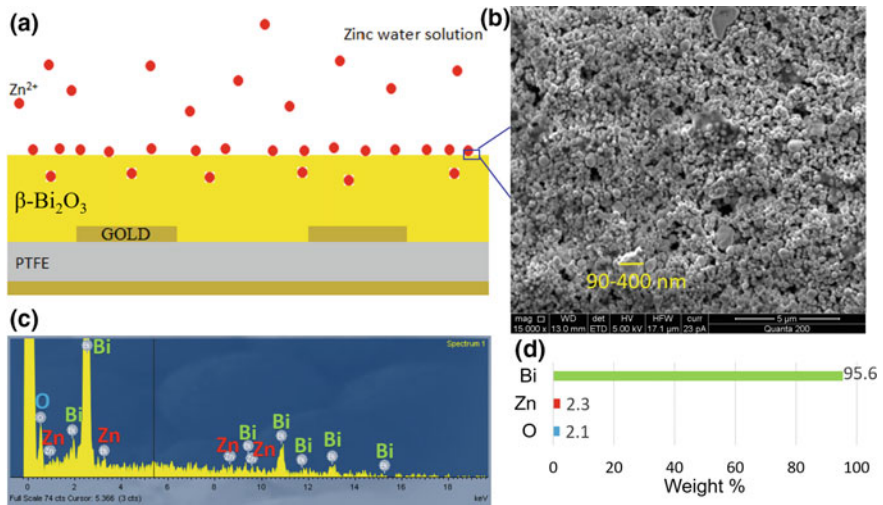
Fig. 5 **a** Partial cross-section of the functionalised sensor illustrating the sorption sensing principle; **b** Scanning electron microscope (SEM) image of the coating after the sorption reaction with the Zn ions where the particle size is highlighted as laying between 90 and 400 nm; **c** Elemental spectra of the film after the adsorption and **d** the elemental weight percentage

environment is reduced when the pH decrease [12]. Therefore, it is probable that the pH influences the Zn adsorption on the β-Bi$_2$O$_3$ based coating.

Figure 5a schematically illustrates the adsorption reaction between the Zn^{2+} ion and the β-Bi$_2$O$_3$ based film. The SEM image of the coating after measurements (Fig. 5b) and the elemental composition spectra and their weight percentage (Fig. 5c, d) obtained with the XRF confirm the presence of Zn on the coating.

The microwave spectra obtained for the Zn solutions at the concentration range 0–100 mg/l were analysed for uncoated and coated sensors with 40 and 60 µm of Bi$_2$O$_3$ based coatings. The higher linear correlation and sensitivity between the S$_{11}$ response and Zn concentration was identified in the frequency range between 2.25 and 2.53 GHz respectively for uncoated sensors and coated sensor with 60 µm coating, as shown in Fig. 6.

Figure 7a shows the timeline responses within 30 min for the Zn solutions measured with microwave spectroscopy with the f-EM sensor with β-Bi$_2$O$_3$ based film with 60 µm thickness at the most pronounced peak (2.53 GHz). Figure 7b and c display the capacitance measurements at 150 Hz performed with the LCR bridge using respectively the same kind of sensor and a coated Ag IDE, with the same 60 µm film, printed on microscope slide in situ and connected with the LCR bridge through crocodile clips. This shows how the S$_{11}$ and C parameters change during the first 10 min and reach stability afterwards. Capacitance and S$_{11}$ tend to increase with Zn concentration, with most of the response occurring within the first 5 min after application of the water sample on the sensor surface; then the signal tends to stabilise by comparison and remains stable beyond 600 s. This demonstrates that the

Fig. 6 Microwave spectra at the frequency range 10 MHz–15 GHz for Zn solutions 0–100 mg/l measured with a 60 μm of Bi_2O_3 based coating: the best linear correlation between Zn concentration and S_{11} response was identified at 2.53 GHz after 10 min
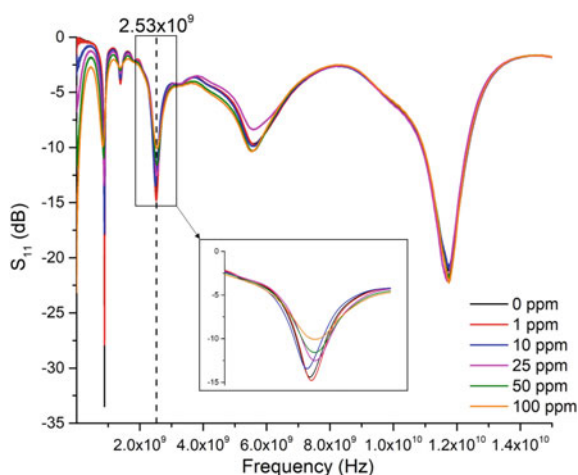
interaction between the functional coating and the Zn ion reach an equilibrium at this point. It is appreciable how adsorption is fast at the beginning of the experiment (first 5 min) and then progressively slows down till the equilibrium is reached.

Figure 8 shows the results obtained with f-EM sensors with 60 μm thickness in the frequency range between 1 and 3 GHz for the range of Zn solutions. A resonant shift occurs depending on the zinc concentration at two resonant frequencies, around 1.38 and 2.53 GHz. The dash-lines express the initial points, after 30 s, the dot-lines after 5 min and the solid-lines after 10 min (equilibrium). The linear correlation for the 60 μm coating for both capacitance and S_{11} response was stronger and the response more sensitive than the 40 μm coating.

Examples of linear correlations obtained for S_{11} (peak, 2.53 GHz) and capacitance at 150 Hz with 60 μm thickness coating at 30, 300 and 600 s are shown in Figs. 9 and 10. Also here is visible how the results with time change are more pronounced in the first part of measurements and minimum after 5 min. As well as the linear correlations between various Zn concentrations are similar between 300 and 600 s for both reflected power ($R^2 = 0.97$) and capacitance ($R^2 = 0.99$). Figure 10a, b compare the response obtained with the same coating thickness (60 μm) on Au IDE EM sensor and the Ag IDE printed on microscope slides. The capacitance and the R^2 are lower with the coated Ag IDE demonstrating that the Au EM sensor performs better for Zn measurements.

The sensor covered with 60 μm of β-Bi_2O_3 based coating result more sensitive than the uncoated sensor and the covered with 40 μm coating. In fact, the change in signal amplitude (expressed as dB/mg/l), at each peak (about 2.5 GHz) is higher for the 60 μm film as shown in Fig. 11 where the data are normalised. The 0 ppm value is cut off because not in line with the diverse Zn concentrations for the measured electrical property of capacitance. This is reflected also in the microwave response (S_{11}) demonstrating the ability of these two methods to identify the presence of the investigated metal.
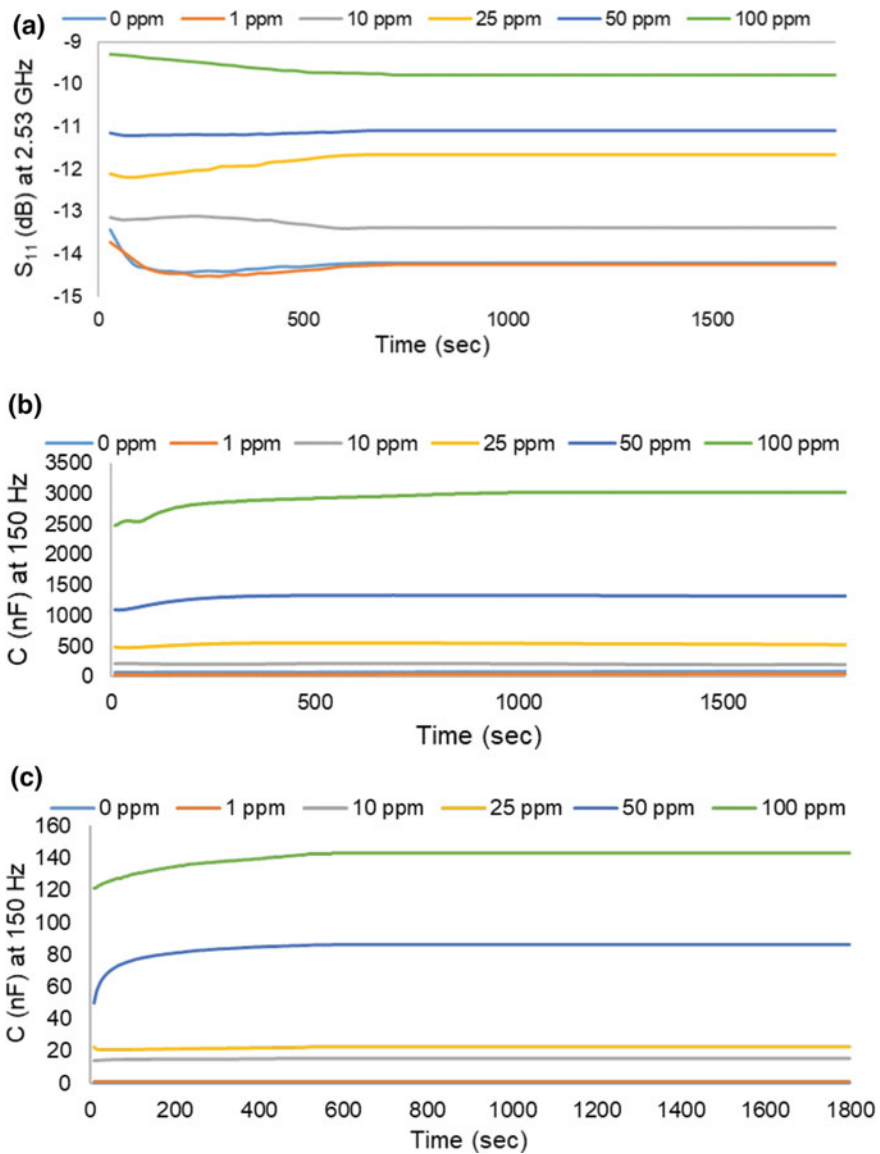
Fig. 7 Timeline response measured with a β-Bi$_2$O$_3$ based film with 60 μm thickness on the Au eight-pair EM sensor measured for 30 min with **a** microwave spectrometry at the peak 2.53 GHz and **b** with the LCR bridge at 150 Hz; **c** shows the timeline capacitance response at the same frequency, with the same thickness of the coating on an Ag IDE screen-printed on a microscope slide
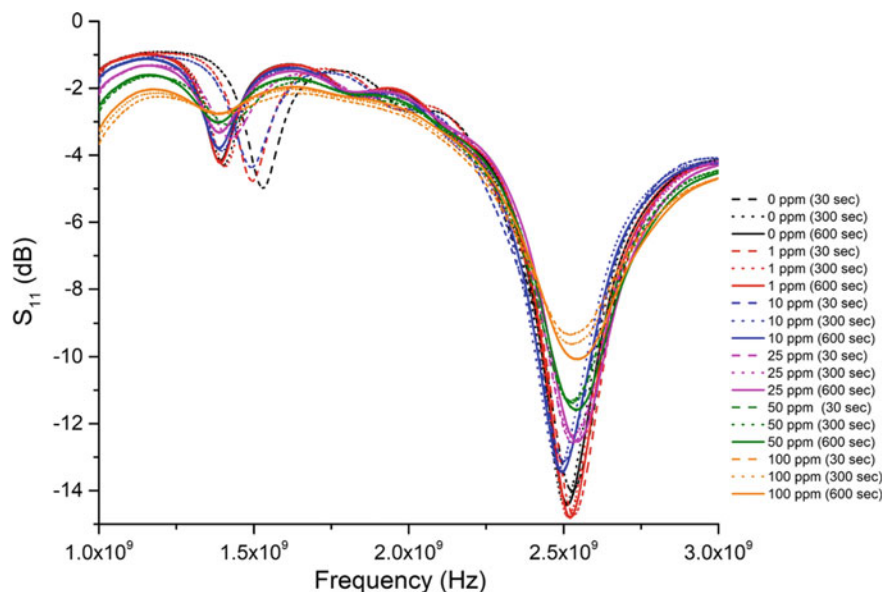
Fig. 8 Microwave output obtained with coated sensors with a β-Bi_2O_3 based thick film with 60 μm; it is been recorded the response obtained after 30 s (dash-lines), after 5 min (dot-lines) and after 10 min (solid-lines)
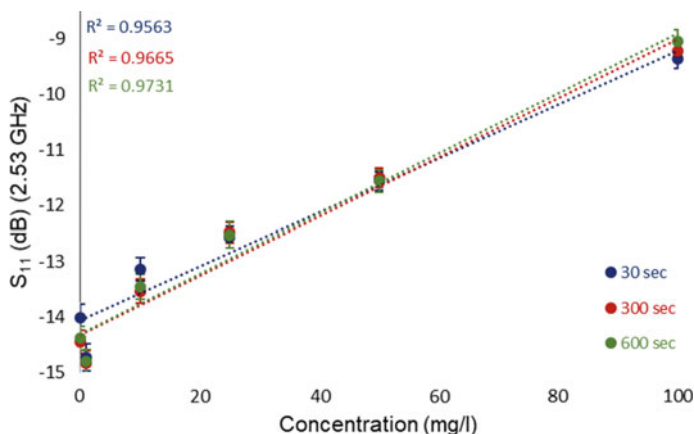

Fig. 9 Linear correlations between reflected power measured at the most pronounced peak (at 2.53 GHz) and Zn concentration at three different times: 30, 300 and 600 s measured with 60 μm thickness of the β-Bi_2O_3 based coating

In the functionalised sensor, the electromagnetic wave propagates in both: the substrate on which gold IDE are printed, and the top β-Bi_2O_3 based thick film. Therefore, the overall propagation will depend on the permittivity of each component
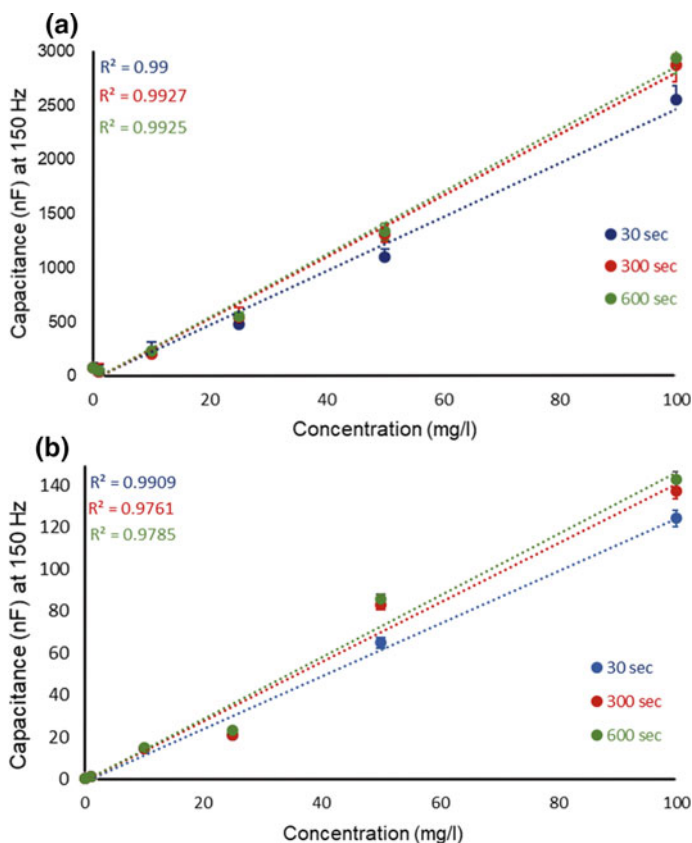
Fig. 10 Linear correlation between capacitance and Zn concentrations measured continuously, every 5 s for 30 min, and illustrate here at three specific times: 30, 300 and 600 s with 60 μm thickness of the film printed on the Au eight-pair IDE sensor (**a**) and on the eight-pair Ag IDE printed on a microscope slide (**b**)

in the system, such as a substrate permittivity and its thickness, and on the sensitive material permittivity, which will change with the adsorption of the zinc in the sensitive layer.

As a result, a continuous measurement protocol must accommodate timing. Regardless the results change with the time and Zn concentration output is related to the reaction time which links to the percentage of adsorption on the film. Consequently, it is more important to consider the relative change and not the absolute value S_{11} or C, exploring relative measurements and to measure samples for the same length of time enabling comparable results.
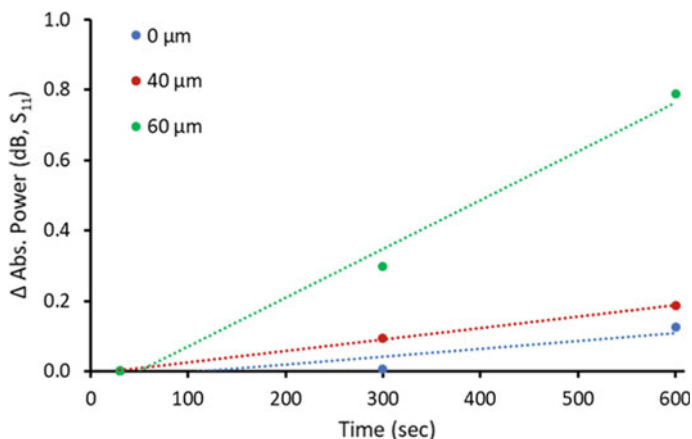
Fig. 11 Sensitivity comparison between an uncoated sensor and two coated sensors with two thicknesses (40 and 60 µm) respectively at each peak (about 2.5 GHz)

Sensor Recovery Time

It was noted that when the sensor is "dry" (unused), the reaction time is longer; when it is "wet" (previously used), it is shorter, although the final results are similar. This is possibly because the solution needs more time to saturate the voids in the film. So, when it is dry the zinc takes longer to be sorbed on the β-Bi_2O_3 tetragonal structure. Consequently, it is necessary to consider the state of the sensor when a water sample is analysed with a thick film sensor.

In this experiment, the sensor recovery time was also evaluated using the LCR bridge and the VNA as the time needed for the response of the sensor to return to the 90% of the original "air spectra". The recovery time was assessed after each measure and each f-EM sensor was rinsed in distilled water. It was recorded as being between 100–150 s, resulting in a return to the air value respectively of 31 pF and 35 pF (Fig. 12) for 40 and 60 µm thickness of films with capacitance measurements. With the microwave measurements, the results are approximately the same, returning to the air spectra after 100–150 s (Fig. 13). The reaction does not alter the coating for many hours of measurements, as also demonstrated by SEM and XRF measurements (Fig. 5b, c). It will begin to alter after about 20 h of continuous monitoring, as described in more detail in the next section.

Reversibility, Stability and Reusability of the Coating

The reversibility, stability and consequent reusability are presumably associated with weak interactions between the sensitive layer and the analyte (physical sorption), very
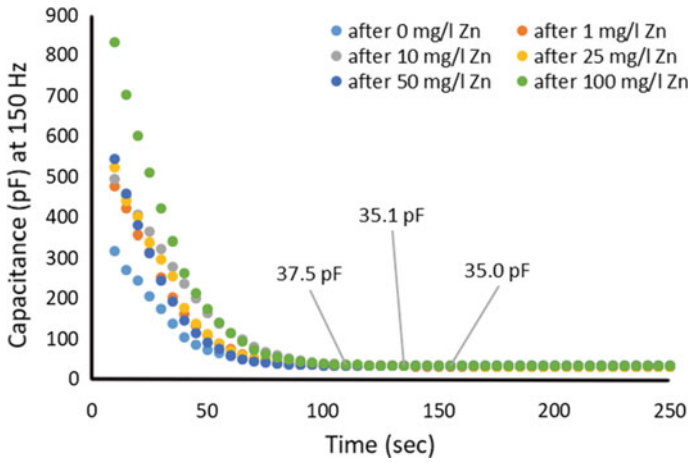
Fig. 12 Recovery time recorded every 5 s with the LCR bridge for the 60 μm thickness which returned to the air value (35 pF) after several Zn solutions measurements at different concentration
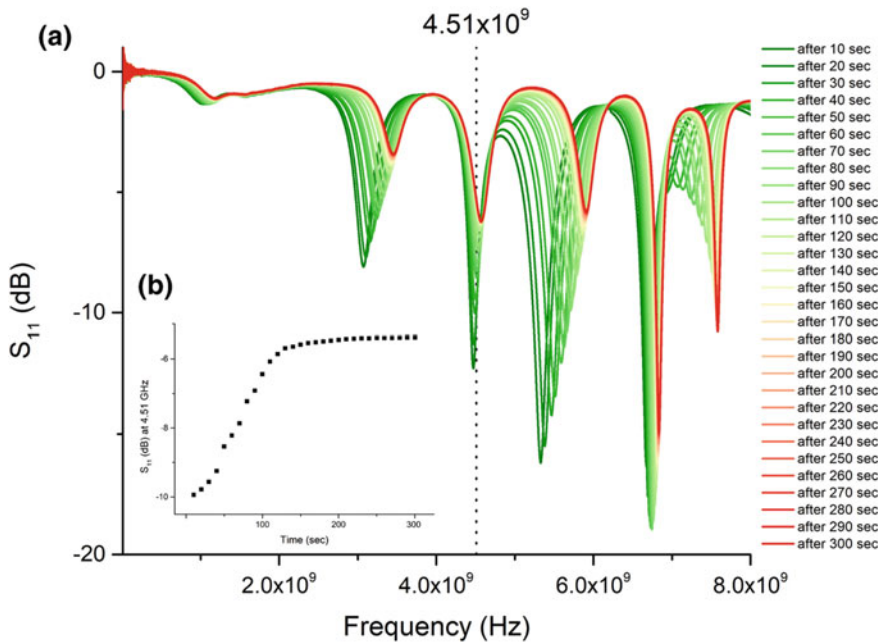

Fig. 13 Example of (**a**) a sensor recovery spectra after 10 mg/l Zn measurements captured every 10 s for 5 min using a VNA. The correlation (**b**) at 4.51 GHz between recovery time and S_{11} response is shown in the bottom left; stability is reached between 100 and 150 s

similar to van der Waals forces, which are the dominant interactions between a large range of metal oxides and cations [45]. Hence, desorption may be the ultimate result. Consequently, there is no degradation of the film for several hours of continuous monitoring and the relative standard deviation (RSD) is<3% for all measurements.

Despite this, after long usage, the film starts to be slightly modified probably because of the 1% HNO_3 of the Zn stock solution, and the consequent formation of bismuth nitrate, mostly with high concentration due to the higher amount of stock solution used for making the standards. This is deducted by a minute change observed in the air spectra and in the coating aspect.

Figure 14 shows the differences of the sensor with 60 µm coating before (a, right) and after (b, left) the sensor is deteriorated and considered disposable, after approximately 20 h of continuous use (see top images). SEM images (bottom) show the morphological surfaces of the coating for the respective sensors: clearly, with long-usage and continuous use, the sensors deteriorate. Specifically, the sensor tends to recover from repeated measurements, but after significant use, this deterioration alters the Zn characteristic response.

Considering reaction time, recovery time and sensor reusability, accomplishing continuous monitoring in situ it will be necessary to use multiple f-EM sensors, with the purpose to cover the time gaps caused by the recovery time of the sensor and obtain a set of comparable and reliable results.

Future Progression

This experimental integration between Bi_2O_3 based thick films and microwave spectroscopy demonstrates the feasibility of using this approach for increasing the performance of Zn detection using microwave spectroscopy. Future experiments will study the possibility to use this novel method for real mine polluted water and multi-metal measurements. Sensor arrays with specific functional materials for diverse toxic pollutants in water will be integrated for simultaneous and continuous monitoring of other metals in water.

Further work would focus on increasing the sensitivity, considering it has been demonstrated in the mg/l range and the EQS for Zn is freshwater is above 0.125 mg/l. However, as an early detection method, the current sensitivity may be acceptable.

Conclusions

This chapter communicates the experimental results of measuring the response and recovery times of functionalised planar type electromagnetic sensors coated with β-Bi_2O_3 for the continuous detection of Zn concentrations in water. A comprehensive set of complementary experiments using electrical and microwave detection methods demonstrate that the state of the sensor and the time of reaction are important for
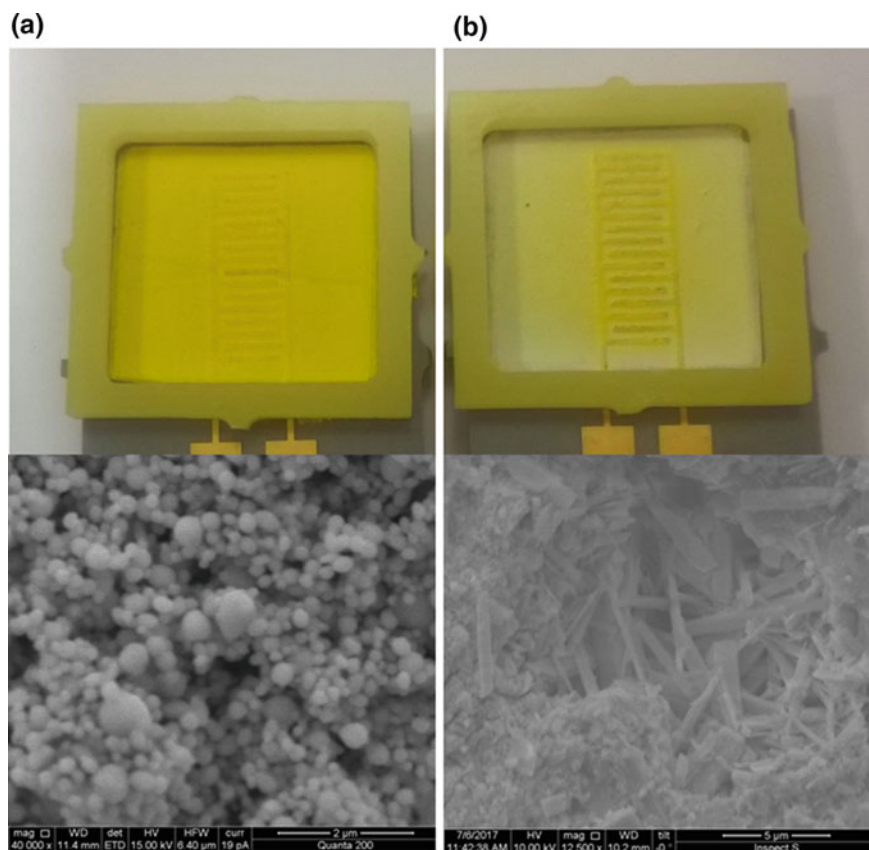
Fig. 14 Photos (top) and related SEM images (bottom) which show the differences between the sensor during the beginning of the measurement (**a**) and after 20 hours (**b**)

reaching a stability between the analysed sample, in this study zinc in water, and the β-Bi$_2$O$_3$ based film. Typically the sensor stabilises 5–10 min after applying a sample, and takes 2–3 min to recover to the original output levels after the sensor is rinsed. This would ideally be faster, but for an unattended system it is still better than sampling and for laboratory-based measurements.

The change in sensor output appears to be reversible (i.e. the sensor recovers), the sensor can be reused, and the output is relatively stable. Re-use should be further investigated since re-use is clearly finite; however, the cost of the sensor would be low in large volumes, so a semi-disposal option is feasible.

This study has confirmed the potential of a novel EM sensing approach combined with functional materials as an alternative method to current offline techniques for Zn concentration monitoring of polluted mine water, and to provide an early warning system for pollution events.

References

1. M.H. Zarifi, A. Gholidoust, M. Abdolrazzaghi, P. Shariaty, Z. Hashisho, M. Daneshmand, Sensitivity enhancement in planar microwave active-resonator using metal organic framework for CO2 detection. Sens. Actuators B Chem. **255,** 1561–1568 (2018)
2. World Health Organization (WHO) and the United Nations Children's Fund (UNICEF), *Progress on Drinking Water, Sanitation and Hygiene: 2017 Update and SDG Baselines*. Geneva (2017)
3. UNICEF and World Health Organization (WHO), *Progress on Sanitation And Drinking Water—2015 Update and MDG Assessment*. Geneva (2015)
4. W.M. Mayes, D. Johnston, H.A.B. Potter, A.P. Jarvis, A national strategy for identification, prioritisation and management of pollution from abandoned non-coal mine sites in England and Wales I. Sci. Total Environ. **407**(21), 5435–5447 (2009)
5. A. Lay-Ekuakille, I. Palamara, D. Caratelli, F. Morabito, Experimental infrared measurements for hydrocarbon pollutant determination in subterranean waters 015103 (2013)
6. P.B. Tchounwou, C.G. Yedjou, A.K. Patlolla, D.J. Sutton, Heavy metals toxicity and the environment. EXS **101**, 133–164 (2012)
7. UK Technical Advisory Group on the Water Framework Directive, UK environmental standards and conditions (phase 1—SR1-2006) (2008)
8. United States Environmental Protection Agency, *Quality Criteria for Water* (Washington, DC 20460: EPA, 1986)
9. P. Rowland, C. Neal, D. Sleep, C. Vincent, P. Scholefield, Chemical quality status of rivers for the water framework directive: a case study of toxic metals in North West England. Water **3**(2), 649 (2011)
10. P. Byrne, P.J. Wood, I. Reid, The impairment of river systems by metal mine contamination: a review including remediation options. Crit. Rev. Environ. Sci. Technol. **42**(19), pp. 2017–2077 (2012)
11. Environment Agency, H1 Annex D-basic surface water discharges, in *Annex D Surface Water Basic*, vol. 2.2 (Environment Agency, Bristol, 2011)
12. K.S. Smith, *Metal sorption on mineral surfaces: an overview with examples relating to mineral deposits* (Environmental Geochemistry of Mineral Deposits. Part A: Processes, Techniques, and Health Issues, 1999), pp. 161–182
13. L.M. Plum, L. Rink, H. Haase, The essential toxin: impact of zinc on human health. Int. J. Environmental Res. Public Health **7**(4), 1342–1365 (2010)
14. A. Léonard, G.B. Gerber, F. Léonard, Mutagenicity, carcinogenicity and teratogenicity of zinc. Mutat. Res. Rev. Genetic Toxicol. **168**(3), 343–353 (1986)
15. United Nations, *Millennium Development Goals (MDGs)* (Salem Press, 2016)
16. R. Altenburger et al., Future water quality monitoring—adapting tools to deal with mixtures of pollutants in water resource management. Sci. Total Environ. **512**, 540–551 (2015)
17. B. Bansod, T. Kumar, R. Thakur, S. Rana, I. Singh, A review on various electrochemical techniques for heavy metal ions detection with different sensing platforms, Biosens. Bioelectron. **94**,. 443–455 (2017)
18. K. Hudson-Edwards, Tackling mine wastes, (in English). Sci. Short Surv. **352**(6283), 288–290 (2016)
19. P. Byrne et al., Water quality impacts and river system recovery following the 2014 Mount Polley mine tailings dam spill, British Columbia, Canada. Appl. Geochem. **91**, 64–74 (2018)

20. G. Pattelli et al., Effects of the November 2012 flood event on the mobilization of Hg from the Mount Amiata mining district to the sediments of the Paglia river basin. Minerals **4**(2), 241 (2014)
21. S.F.L. Lynch, L.C. Batty, P. Byrne, Critical control of flooding and draining sequences on the environmental risk of Zn-contaminated riverbank sediments, J. Soils Sedim. (2017)
22. R. Cidu, F. Frau, S. Da Pelo, Drainage at abandoned mine sites: natural attenuation of contaminants in different seasons. Mine Water Environ. J. Artic. **30**(2), 113–126 (2011)
23. P. Byrne, I. Reid, P.J. Wood, Stormflow hydrochemistry of a river draining an abandoned metal mine: the Afon Twymyn, central Wales. Environ. Monit. Assess. J. Artic. **185**(3), 2817–2832 (2013)
24. A. Jones, M. Rogerson, G. Greenway, H.A.B. Potter, W.M. Mayes, Mine water geochemistry and metal flux in a major historic Pb-Zn-F orefield, the Yorkshire Pennines, UK. Environ. Sci. Pollut. Res. **20**(11), 7570–7581 (2013)
25. M.B. Gumpu, S. Sethuraman, U.M. Krishnan, J.B.B. Rayappan, A review on detection of heavy metal ions in water—An electrochemical approach, Sens. Actuators B Chem. **213**, 515–533 (2015)
26. Z. Kovacs et al., Water spectral pattern as holistic marker for water quality monitoring, Talanta **147**, 598–608 (2016)
27. J. Iqbal, D.U. Yiping, F. Howari, M. Bataineh, N. Muhammad, A. Rahim, Simultaneous enrichment and on-line detection of low-concentration copper, cobalt, and nickel ions in water by near-infrared diffuse reflectance spectroscopy combined with chemometrics. J. AOAC Int. Artic. **100**(2), 560–565 (2017)
28. A. Mason et al., Theoretical basis and application for measuring pork loin drip loss using microwave spectroscopy, Sensors **16**(2), 182 (13 pp.) (2016)
29. O. Korostynska, A. Mason, M. Ortoneda-Pedrola, A. Al-Shamma'a, Electromagnetic wave sensing of NO3 and COD concentrations for real-time environmental and industrial monitoring. Sens. Actuators B Chem. **198**, 49–54 (2014)
30. L.F. Chen, C.K. Ong, C.P. Neo, V.V. Varadan, V.K. Varadan, Planar-circuit methods, in *Microwave Electronics* (Wiley, 2005), pp. 288–322
31. M.H. Zarifi, M. Daneshmand, Liquid sensing in aquatic environment using high quality planar microwave resonator. Sens. Actuators B Chem. **225**(Supplement C), 517–521 (2016)
32. S. Cashman, O. Korostynska, A. Shaw, P. Lisboa, L. Conroy, Detecting the presence and concentration of nitrate in water using microwave spectroscopy, IEEE Sens. J. **PP**(99), 1–1 (2017)
33. A. Chahadih, P.Y. Cresson, Z. Hamouda, S. Gu, C. Mismer, T. Lasri, Microwave/microfluidic sensor fabricated on a flexible kapton substrate for complex permittivity characterization of liquids. Sens. Actuators A Phys. **229**(Supplement C), 128–135 (2015)
34. M.H. Zarifi, B. Wiltshire, N. Mahdi, P. Kar, K. Shankar, M. Daneshmand, Ultraviolet sensing using TiO2 nanotube integrated high resolution planar microwave resonator device. Nanoscale (2018)
35. M.H. Zarifi, H. Sadabadi, S.H. Hejazi, M. Daneshmand, A. Sanati-Nezhad, Noncontact and nonintrusive microwave-microfluidic flow sensor for energy and biomedical engineering. Sci. Rep. (2017)
36. M.E.E. Alahi, A. Nag, S.C. Mukhopadhyay, L. Burkitt, A temperature-compensated graphene sensor for nitrate monitoring in real-time application. Sens. Actuators A Phys. **269**(Supplement C), 79–90 (2018)
37. A. Rydosz, E. Maciak, K. Wincza, S. Gruszczynski, Microwave-based sensors with phthalocyanine films for acetone, ethanol and methanol detection. Sens. Actuators B Chem. **237**, 876–886 (2016)
38. A. Mason et al., Noninvasive *In-Situ* measurement of blood lactate using microwave sensors. IEEE Trans. Biomed. Eng. **65**(3), 698–705 (2018)
39. M.H. Zarifi, S. Farsinezhad, M. Abdolrazzaghi, M. Daneshmand, K. Shankar, Selective microwave sensors exploiting the interaction of analytes with trap states in TiO2 nanotube arrays. Nanoscale **8**(14), 7466–7473 (2016). https://doi.org/10.1039/C5NR06567D

40. A. Bogner, C. Steiner, S. Walter, J. Kita, G. Hagen, R. Moos, Planar microstrip ring resonators for microwave-based gas sensing: design aspects and initial transducers for humidity and ammonia sensing. Sensors **17**(10), 2422 (2017)
41. A. Azmi et al., Performance of coating materials on planar electromagnetic sensing array to detect water contamination. IEEE Sens. J. **17**(16), 5244–5251 (2017)
42. R. Igreja, C.J. Dias, Dielectric response of interdigital chemocapacitors: the role of the sensitive layer thickness. Sens. Actuators B Chem. **115**(1), 69–78 (2006)
43. E. Reimhult, F. Höök, Design of surface modifications for nanoscale sensor applications. Sensors (Basel, Switzerland) **15**(1), 1635–1675 (2015)
44. G. Aragay, J. Pons, A. Merkoci, Recent trends in macro-, micro-, and nanomaterial-based tools and strategies for heavy-metal detection. Chem. Rev. **111**(5), 3433–3458 (2011)
45. S. Sen Gupta, K.G. Bhattacharyya, Kinetics of adsorption of metal ions on inorganic materials: a review. Adv. Colloid Interface Sci. **162**(1–2), 39–58 (2011)
46. L. Cui, J. Wu, H. Ju, Electrochemical sensing of heavy metal ions with inorganic, organic and bio-materials. Biosens. Bioelectron. **63**, 276–286 (2015)
47. P.K. Chatterjee, A.K. SenGupta, Toxic metal sensing through novel use of hybrid inorganic and polymeric ion-exchangers. Solv. Extr. Ion Exch. **29**(3), 398–420 (2011)
48. V. Ferrari, M. Prudenziati, 8—Printed thick-film capacitive sensors, in *Printed Films*: (Woodhead Publishing, 2012), pp. 193–220
49. M. Prudenziati, M. Prudenziati (eds.) *Handbook of Sensors and Actuators*, 1st ed. (Thick Film Sensors) (Amsterdam, 1994)
50. M. Prudenziati, J. Hormadaly, 1—Technologies for printed films, in *Printed Films* (Woodhead Publishing, 2012), pp. 3–29
51. M. Kohl, G. Veltl, M. Busse, Printed sensors produced via thick-film technology for the use in monitoring applications. Procedia Technol. **15**, 107–113 (2014)
52. B. Yosypchuk, J. Barek, Analytical applications of solid and paste amalgam electrodes. Crit. Rev. Anal. Chem. **39**(3), 189–203 (2009)
53. J. Hormadaly, M. Prudenziati, 2—Materials for printed films, in *Printed Films* (Woodhead Publishing, 2012), pp. 30–62
54. G.-J. Lee, H.-M. Lee, C.-K. Rhee, Bismuth nano-powder electrode for trace analysis of heavy metals using anodic stripping voltammetry. Electrochem. Commun. **9**(10), 2514–2518 (2007)
55. I. Švancara, C. Prior, S.B. Hočevar, J. Wang, A decade with bismuth-based electrodes in electroanalysis. Electroanalysis **22**(13), 1405–1420 (2010)
56. R.O. Kadara, N. Jenkinson, C.E. Banks, Disposable bismuth oxide screen printed electrodes for the high throughput screening of heavy metals. Electroanalysis **21**(22), 2410–2414 (2009)
57. A.O. Dada, A. Olalekan, A. Olatunya, D.O. Dada, Langmuir, Freundlich, Temkin and Dubinin-Radushkevich isotherms studies of equilibrium sorption of Zn^{2+} unto phosphoric acid modified rice husk. IOSR J. Appl. Chem. **3**(1), 38–45 (2012)